Earth and Planetary Science Letters 473 (2017) 131–140

Contents lists available at ScienceDirect

Earth and Planetary Science Letters

www.elsevier.com/locate/epsl

Slow fault propagation in serpentinite under conditions of high pore fluid pressure

Melodie E. French [a,b,*], Wenlu Zhu [b]

[a] Department of Earth, Environmental and Planetary Sciences, Rice University, United States
[b] Department of Geology, University of Maryland, College Park, United States

ARTICLE INFO

Article history:
Received 8 March 2017
Received in revised form 1 June 2017
Accepted 3 June 2017
Available online xxxx
Editor: P. Shearer

Keywords:
faulting
experimental rock deformation
slow slip
fluid pressure
microstructures

ABSTRACT

The rupture, localization, and slip of faults in serpentinite were studied under varying pore fluid pressure conditions to understand deformation mechanisms potentially responsible for slow slip in fault zones. Experiments were conducted at a constant effective confining pressure of 10 MPa and under pore fluid pressures from 0 to 120 MPa and at temperatures from 23 to 110 °C. With no fluid pressure, faulting occurs rapidly and audibly, and the duration of failure increases monotonically with increasing fluid pressure and temperature. Although non-dilatant during initial strain hardening, the serpentinite dilates during strain weakening concomitant with fault rupture and slip. Non-dilatant strain hardening occurs by microcracking along serpentine basal planes and grain boundaries and rarely in mode I orientations, consistent with previous studies. Dilatant fault rupture produces a network of transgranular shear fractures in conjugate orientations, generally with one dominant fracture. Structural observations show that as fluid pressure increases, the number of transgranular fractures increases. We propose that when faulting occurs over a distributed zone rather than a pre-existing principal slip surface, dilatant hardening causes deformation to migrate. This process causes an increase in slip weakening distance and fracture energy at elevated fluid pressures that can lead to more stable failure. Further, thermally-activated processes caused deformation at propagating crack tips, which also increases the slip weakening distance and the effective fracture energy with increasing temperature. Given the geologic settings for slow slip, our results indicate that high fluid pressure, distributed deformation, and thermally-activated processes may all contribute to slow fault rupture and slip.

1. Introduction

Current physical models reproduce well fault slip that occurs as steady creep or undergoes earthquake cycles, and these models are consistent with both geological and laboratory based studies of fault rocks (Scholz, 2002). There are still a number of competing hypotheses, however, for the episodic 'slow slip' that is observed in subduction zones and inferred along the deep extent of the San Andreas Fault (Dragert et al., 2001; Shelly et al., 2009). Whereas earthquake ruptures propagate at rates on the order of elastic wave speeds with fault slip on the order of m/s, slow slip events propagate on the order of ~10 km/day with fault slip on the order of 0.01 μm/s (Schwartz and Rokosky, 2007). Hypotheses for the mechanisms of fault rupture and slip aim to reconcile the self-sustaining nature of slow slip with the fact that propagation and slip do not accelerate to earthquake speeds.

In most numerical simulations of faulting, it is assumed that slip is localized along a pre-existing discontinuity weaker than the surrounding damage rock, motivated largely by field studies that show high-displacement faults develop localized slip surfaces mm to cm thick (Chester and Chester, 1998). Stability analyses show that whether slip rates become unbounded resulting in an earthquake is controlled by both the constitutive behavior of fault shear stress, often expressed in terms of rate- and state-friction, and the stiffness of the system (Gu et al., 1984). Many prominent hypotheses for the causes of slow slip propose that the constitutive properties promote competing tendencies between slip acceleration and deceleration (Rubin, 2011; Segall and Bradley, 2012; Ikari et al., 2013), or a system stiffness at the boundary between promoting unstable and stable slip (Rubin, 2008; Leeman et al., 2016).

We attempt to reconcile hypotheses based on stability arguments with the mechanical properties, rock structures, and extrinsic variables that exist at the conditions of slow slip. Constraining physical properties at slow slip conditions is the subject of current work, but we target a few parameters that seem to correlate strongly with the conditions at locations where slow slip is ob-

* Corresponding author.
E-mail address: mefrench@rice.edu (M.E. French).

http://dx.doi.org/10.1016/j.epsl.2017.06.009
0012-821X/

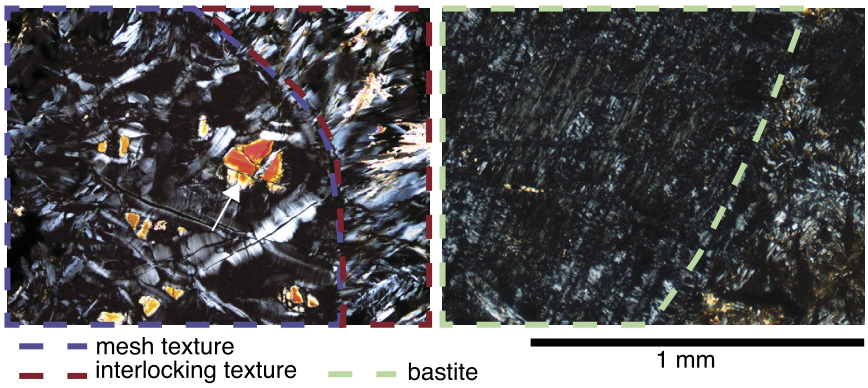

Fig. 1. Cross-polarized light photomicrographs of the Coast Ranges antigorite serpentinite showing the three primary textures observed. The white arrow indicates a relict olivine grain.

served. First, slow slip is reported in several subduction zones, near transitions between seismogenic and creeping regions of the fault, and is inferred to occur along the deep extent of the San Andreas Fault (Schwartz and Rokosky, 2007; Shelly et al., 2009). Although the exact lithology of the fault rocks that host slow slip are not known in any location, slow slip events and associated tremor have been relocated to the plate boundary interface in both subduction zones and along the San Andreas Fault where phyllosilicate phases are common (Dragert et al., 2001; Wech and Creager, 2007; Fagereng and Diener, 2011). Second, fault zones in phyllosilicate-rich rocks and seismic to aseismic transitional regions both tend to correlate with fault strain that is distributed over tens of meters or more rather than localized to principal slip surfaces mm to cm thick (Rowe et al., 2013; Fagereng et al., 2014). Finally, geophysical observations indicate that pore fluid pressure in active fault zones may be very high, and near-lithostatic in regions that exhibit slow slip (Kodaira et al., 2004; Shelly et al., 2006; Audet et al., 2010). As a result, one prominent hypothesis to explain the occurrence of slow slip calls upon high pore fluid pressure as a cause through a process known as 'dilatant hardening' (Segall et al., 2010).

During brittle deformation, mode I microcracks cause dilation of pore space resulting in a concomitant decrease in pore fluid pressure (Brace and Bombolakis, 1963). Dilatant hardening is the process by which such transient changes in fluid pressure cause an increase in strength, because the shear strength along a fault, τ, increases proportional to the effective normal stress, $\sigma_n - \alpha P_f$, where σ_n is the total normal stress and P_f is the pore fluid pressure, and α is the pore fluid pressure coefficient and is often found to be ≈ 1 for brittle faulting. Analytical and numerical models show that dilatancy can cause a delay between the initiation of strain weakening and rapid slip, but they do not support dilatant hardening as a mechanism for limiting fault slip rates throughout an entire event (Rudnicki, 1984). Furthermore, dilatancy due to mode I microcracking is negligible in phyllosilicate-rich lithologies because cracks preferentially develop as shear and mixed mode cracks parallel to the phyllosilicate basal plane (Escartin et al., 1997). As a result, whether high pore fluid pressures and dilatant hardening contribute to slow slip in serpentinite and other phyllosilicate-rich rocks common to the geologic environment of slow slip is unknown.

We faulted intact cores of serpentinite under conditions of high pore fluid pressure in a triaxial rock deformation apparatus to test for and characterize dilatancy hardening in phyllosilicate-rich fault rocks. We chose to test intact samples to measure the role that microcrack growth and coalescence have on localization of deformation and fault slip under conditions of high pore fluid pressure. Although the magnitude of cohesion of intact serpentinite is much greater than that of plate boundary fault rocks, the processes of crack growth and coalescence that occur in these experiments are representative of those that occur in-situ. These tests compliment previous work that investigate slip along incohesive faults under conditions of high pore fluid pressure (Bartlow et al., 2012; Okazaki et al., 2013; French et al., 2016).

2. Materials and methods

2.1. Serpentinite

We investigate faulting in an antigorite-rich serpentinite from the Coast Ranges of California, USA. The serpentinitized harzburgite has pseudomorphic texture with relict grains of olivine and orthopyroxene. The composition of the serpentinite was determined using a combination of X-ray diffraction (XRD) on a powdered sample and analysis of back-scattered electron (BSE) images of 4 samples. The average and standard deviation volumetric composition of the Coast Range serpentinite is: 86 ± 8% antigorite, 7 ± 6% olivine and orthopyroxene, and 7 ± 3% oxides.

The antigorite occurs in three primary textures (Fig. 1). Antigorite that partially or completely replaces olivine and orthopyroxene grains occurs in mesh texture and bastite texture, respectively. We also observe an interpenetrating texture that separates and surrounds regions of mesh texture. Overall, there is no crystallographic preferred orientation (CPO) of the antigorite grains, but replacement textures result in local CPOs on the scale of the original peridotite grain size (~1 mm).

2.2. Deformation experiments

We conducted 9 axial compression experiments on intact serpentinite cores 25.4 mm in diameter and 50.8 mm in length using a triaxial deformation apparatus (Table 1). The cores were faulted under axial compression at a displacement rate of 0.1 μm/s (strain rate of 2.4×10^{-6}) and confining pressure was held constant. To isolate the effects of pore fluid pressure on the strength and rupture properties, the experiments were conducted at the same effective confining pressure $\sigma_3' = \sigma_3 - \alpha P_f = 10$ MPa, assuming that $\alpha \approx 1$, but at fluid pressures, P_f, of 0, 60, or 120 MPa with corresponding confining pressures, σ_3, of 10, 70, or 130 MPa. For comparison with the serpentinite, we also conducted a set of experiments on the Sierra White granite at room temperature and at 0 and 120 MPa pore fluid pressure.

The serpentinite was faulted at temperatures from 23 to 110 °C. Temperature was controlled by an internal furnace. The greatest uncertainty in reported temperature is caused by a gradient in temperature along the sample axis that is symmetric about the center; there is a ~5% variation from maximum temperature at the core center to a minimum at either end.